

Damage Detection in a Geometrically Constrained Area ¹

E.D. Swenson² and S.R. Soni³

Abstract: A "hot-spot" structural health monitoring (SHM) approach that uses lead zirconate titanate (PZT) sensor pairs to generate and sense Lamb waves is evaluated on a test article that accurately represents the complex geometry of a relatively inaccessible bulkhead section of an existing aircraft. This work is motivated by the fact that fatigue cracks have been known to propagate in this particular bulkhead in several aircraft. In order to simulate damage, electrical discharge machine (EDM) cuts are made to simulate real cracks in a test article. Because the damage occurs in a region of restricted geometry, PZT sensors must be placed in close proximity to each other, but on opposing sides of the expected crack. The close proximity of the piezoelectric sensors and restricted geometry create challenges in determining which portion of the collected response should be analyzed. The first approach evaluated is a tuning approach where specific excitation frequencies are chosen based on the relative S_0 and A_0 Lamb wave mode amplitudes. Theoretical time of arrival window lengths for the S_0 and A_0 Lamb wave modes are reduced in size to minimize the contribution of reflected wave energy. The second approach involves evaluating responses over a wide range of excitation frequencies in combination with only evaluating the responses in the dominant mode's theoretical time of arrival window. A simple damage metric is applied to demonstrate that the presence of cracks can be detected as well as the length can be roughly approximated. This approach is further validated with laser vibrometry scans of the test article in both healthy and damaged states.

Keywords: Damage detection, structural health monitoring, SHM, PZT, Lamb wave, laser vibrometry.

¹ The views expressed in this article are those of the authors and do not reflect the official policy or position of the Air Force, Department of Defense or the U.S. Government

² Department of Aeronautics and Astronautics, U.S. Air Force Institute of Technology, Wright-Patterson Air Force Base, OH, USA.

³ Department of Systems Engineering and Management, U.S. Air Force Institute of Technology, Wright-Patterson Air Force Base, OH, USA.

1 Introduction

The United States Air Force (USAF) has an aging aircraft fleet with high operational demands that requires mission success in a variety of environmental conditions. The USAF has increased its demand for sustainment of aging aircraft (over 25 years) in service, and knowledge of a system's structural integrity is of vital importance in determining the operational status of an aircraft [Mal (2004)]. Structural integrity status is usually obtained through scheduled maintenance inspections, which are time consuming and expensive because they usually require disassembly of a structure so visual or other types of non-destructive inspections can be made. The information gathered on a system's structural integrity through SHM detection methods should result in reduced costly maintenance inspections, enhanced safety, and system failure predictions [Kessler (2002)].

Visual or other types of non-destructive inspections can inflict unnecessary damage to a healthy structure. By performing condition based maintenance (CBM) - maintenance performed only when problems are known to exist - costly unnecessary scheduled inspections would be reduced. According to Mal, over 25% of an aircraft's life cycle cost is due to maintenance and inspections of the airframe [Mal (2004)]. Therefore, the goal of this research is to evaluate an existing "hot spot" SHM approach on an aircraft bulkhead that is relatively inaccessible by maintenance technicians and has been known to have fatigue cracking that compromises structural integrity. For example, Fig. 1 shows the location of a crack in an aircraft titanium bulkhead. The SHM approach being evaluated uses piezoelectric generated Lamb waves to detect damage and is evaluated on a test article that has EDM cuts that represent cracks. This paper is organized as follows.

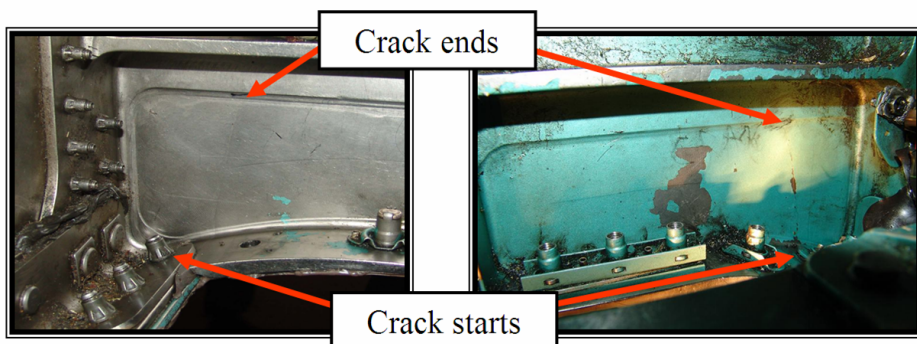


Figure 1: Photograph of front and back views of a cracked aircraft titanium bulkhead

First, a discussion on the background is provided followed by a presentation on the test article that was designed to accurately represent the actual aircraft bulkhead with damage representative of the actual damage. Next, the experimental test setup and procedures are presented. Lastly, the results of this study are presented followed by conclusions.

2 Background

Because Lamb wave theory has been fully documented in numerous text books and articles, it will not be reproduced in this paper other than the relevant features of Lamb waves directly related to the challenges of this problem. There have been several focused studies on SHM systems specifically for aircraft. Swenson and Crider [Swenson and Crider (2007)] conducted the initial work in evaluating the damage detection approach being evaluated in this research. Kessler, Amaratunga, and Wardle [Kessler, Amaratunga and Wardle (2005)] studied sensor durability and discussed various durability standards for commercial and military aircraft components and how they relate to aircraft SHM systems. Kessler and Shim [Kessler and Shim (2005)] created an SHM system specifically designed for aircraft systems called the Monitoring & Evaluation Technology Integration Disk (M.E.T.I.-Disk) and demonstrated its capability to detect the presence and location of damage. Lu, Ye, Su, and Yang [Lu, Ye, Su and Yang (2008)] studied the interaction of Lamb wave modes at varying frequencies with a through-thickness crack in aluminum plates at various angles. They found that wave scattering from a crack leads to complicated transmission, reflection, and diffraction accompanied with mode conversion. To assist in clear identification of crack-scattered waves, they applied a dual PZT actuation scheme to generate S_0 modes only.

In the last decade, there have been many studies that have included the use of laser vibrometers to measure Lamb waves and detect damage. Staszewski, Lee, Mallet, and Scarpa [Staszewski, Lee, Mallet and Scarpa (2004)] demonstrated the use of a laser velocimeter to measure Lamb waves and applied enhanced data smoothing and filtering procedures. They validated their results using classical piezoceramic-based sensing and numerical simulations. In their second paper [Mallet, Lee, Staszewski and Scarpa (2004)], they applied laser vibrometry to damage detection and demonstrated its potential for detecting the presence and location of damage in structures. In conjunction with Leong [Leong, Staszewski, Lee and Scarpa (2005)], the authors conducted fatigue tests in order to initiate and grow a crack and detected the cracks using PZT generated Lamb waves using a laser vibrometer. In this last paper, they demonstrated that laser vibrometers can be used to detect fatigue cracks in metallic structures. Hutchins, Lundgren, and Palmer [Hutchins, Lundgren and Palmer (1989)] generated and detected Lamb waves using a laser vibrometer and

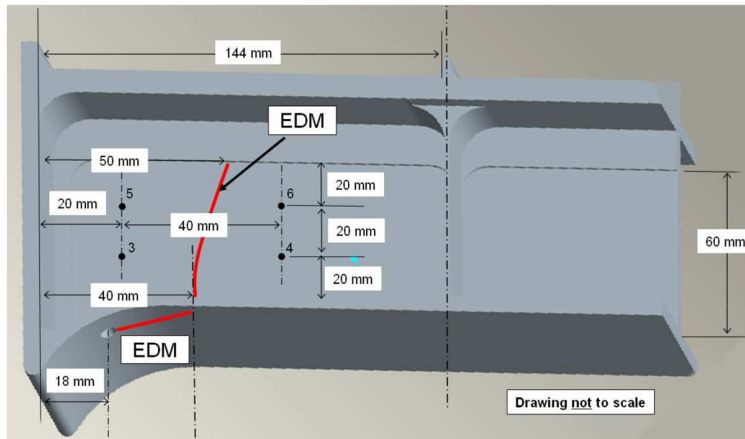


Figure 2: Three-dimensional (3D) computer-aided drawing (CAD) of the aircraft bulkhead test article and piezoelectric sensor placement

signal processing techniques to determine the dispersion characteristics of the A_0 and S_0 modes in order to estimate both the thickness and elastic constants of their samples. Gao, Glorieuxa, and Thoena [Gao, Glorieuxa and Thoena (2003)] measured Lamb waves in a thin copper plate using a laser vibrometer to detect the various Lamb wave modes and determined the material thickness, wave bulk velocities, and material elastic constants.

3 Test Article Description

Testing could not be performed on an actual aircraft. Therefore, a test article has been milled from 6061-T6 aluminum with nearly identical dimensions as the original aircraft bulkhead (see Fig. 2). Aluminum is a suitable substitute for titanium for this test because the theoretical dispersive properties of Lamb waves in certain grades of titanium and aluminum are quite similar over a wide range of frequencies [Crider (2007)].

To simulate a crack representative of the actual damage, a series of EDM cuts are made with a 0.254 mm diameter wire resulting in a 0.305 mm wide, full-penetration cut. The cuts are accomplished over three intervals with data collection between each interval. The first cut begins at the lower horizontal stiffener hole and ends 15 mm up the vertical stiffener and 40 mm from the left vertical stiffener (see Fig. 3). The second cut begins at 35 mm from the left vertical stiffener and 5 mm above the lower horizontal stiffener and ends 43 mm from the left vertical stiffener and 30 mm above the lower horizontal stiffener. For the second cut, an EDM wire

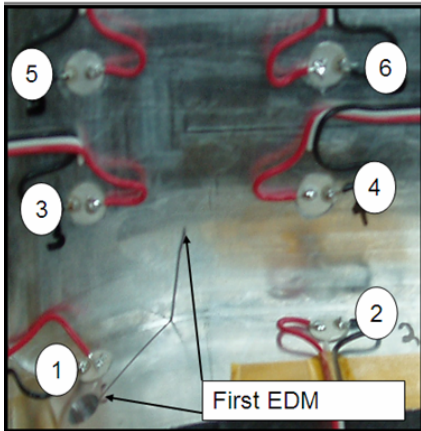


Figure 3: PZT locations for Sensors 1 through 6 with first EDM cut shown

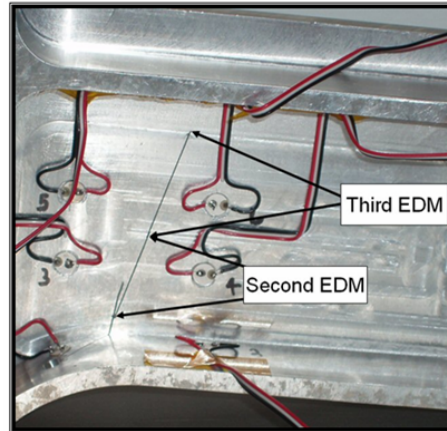


Figure 4: Second and third EDM cuts shown

clearance hole is drilled to ensure the second cut is tied into the first cut. The third cut continues where the second cut ends and terminates at the start of the upper thickness change and 50 mm from the left stiffener (shown in Fig. 4).

A total of six 6.35 mm diameter American Piezo Ceramics (APC) 850 piezoelectric sensors are attached to the test article using M-Bond 200 adhesive (shown in Fig. 3). Sensors 1 and 2 are attached on the 6 mm thick lower horizontal stiffener. The horizontal stiffener is 24 mm wide and the hole from which the crack initiates is 6 mm in diameter and centered on the stiffener. There is a span of 9 mm between the hole and the bulkhead vertical stiffener. Sensor 1 is centered on the 9 mm span, and Sensor 2 is attached directly across from Sensor 1. The remaining four piezoelectric sensors, Sensors 3 through 6, are attached on the 3 mm thick vertical stiffener at the locations shown in Figs. 2 and 3.

The intent of the placement of Sensors 1 and 2 is to detect a crack as it propagates from the horizontal stiffener hole across the horizontal stiffener (see Fig. 3). Sensors 3 and 4 are placed to detect damage as the crack starts to propagate up the vertical stiffener. Finally, Sensors 5 and 6 are placed to detect damage as a crack continues to propagate toward the top of the vertical stiffener.

4 Experimental Tests

The SHM approach is primarily evaluated by both comparing signals collected from discrete PZT sensors and is further validated by laser vibrometry scan data

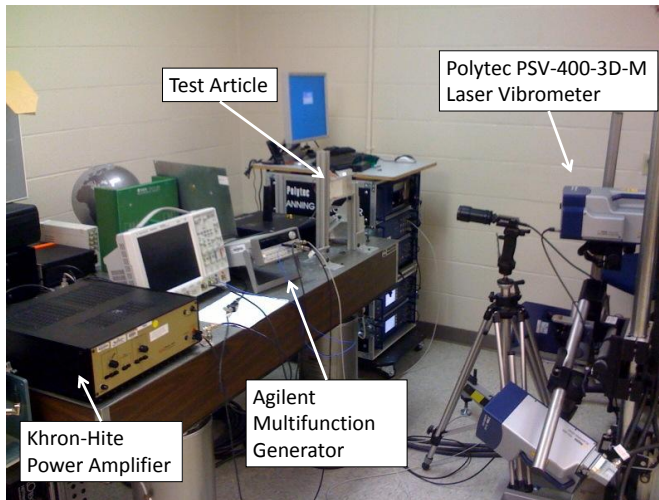


Figure 5: Photograph of the laser vibrometer test setup

of both the damaged and undamaged test articles. The use of a laser vibrometer in this research is not intended for actual damage detection. Instead, this relatively expensive and fairly complex lab instrument is used to attain higher levels of understanding of Lamb wave interaction with the structure and damage.

A Polytec PSV-400-3D-M high frequency scanning laser vibrometer is used in a 1D mode to measure the out-of-plane surface velocities from the Doppler shift in the return signal (see Fig. 5). The 3D capabilities of this instrument could not be used because the upper and lower horizontal stiffeners would block lasers that are not normal to the measurement surface. A complete scan takes on average 3.5 hours to collect measurements from 13,197 locations which are each measured 20 times at a 2.56 MHz sampling rate and averaged to minimize the effects of noise. There is a 50 ms delay between each collection to allow input excitations to decay to levels similar to the ambient noise. Only Sensor 6 is used to excite Lamb waves in this portion of the experiment primarily because Sensor 6 is centrally located. A multifunction generator and Khron-Hite model 7500 1MHz wideband power amplifier created 100 volt peak-to-peak 80 and 250 kHz excitation signals. The resulting Lamb waves were easily measured because a light dispersive coating of Magnaflux SKD-S2 SpotCheck Developer was applied to the scan area which yields a stronger laser return signal. Each complete scan clearly shows the interaction of Lamb waves with the structural complexities of the test article which reveals why interpreting PZT signals is challenging especially in test articles with restricted geometry. The laser scan portion of this experiment consists of two phases, a scan

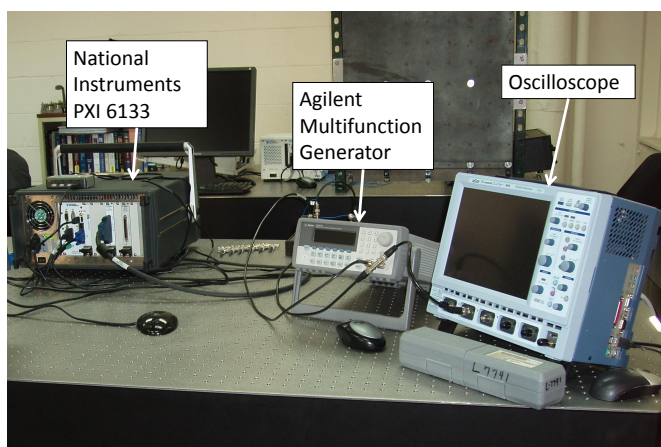


Figure 6: Photograph of the discrete PZT experimental setup

of the healthy structure and a scan of the damaged structure corresponding to the third of the three incremental EDM cuts.

For the discrete PZT sensor part of this experiment, a multifunction generator is used to generate $5\frac{1}{2}$ cycle Hanning-windowed sine wave excitation signals in a frequency range of 50 to 600 kHz in increments of 10 kHz (see Fig. 6). National Instruments (NI) PXI 6133 data acquisition cards are controlled by a data acquisition computer in a LabVIEW environment to collect the response data. At a sampling rate of 2.5 MHz, 1,000 samples are collected resulting in a total sampling period of $400\ \mu\text{s}$ for each measurement. Because piezoelectric sensors can be used for both actuating and sensing Lamb waves, a pitch-catch approach is used where the structure is excited at one sensor and the response measured at another. In this portion of the experiment, all six piezoelectric sensors are each excited individually, and responses are collected from the remaining five sensors. There are four phases of data collection and the first is collecting responses from a healthy structure and the remaining three phases are for the three damaged structure data collection phases. The three damage collection phases correspond to the three incremental EDM cuts. Because the EDM machine uses pressurized distilled water during cutting, there was a concern that the six attached piezoelectric sensors could have been damaged during cutting. Therefore, an Agilent 4294 Precision Impedance Analyzer was used to determine if any of the six piezoelectric sensors were damaged by the EDM process. Fortunately, no detectable changes were measured in the imaginary part of the complex admittance of the impedance measurement [Park, Farrar, Rutherford

and Robertson (2006)].

4.1 Results

The actual damage in the aircraft bulkhead occurs in a section of fairly complex geometry, as shown in Fig. 2. Since the approach taken here focuses on evaluating response signals arriving directly from the excitation sensor, the piezoelectric sensors have been mounted close to each other in order to minimize the effects of reflected signals. As a result of the piezoelectric sensors being placed only 40 mm apart, both the S_0 and A_0 packets arrive within several microseconds of each other. For example, the arrival times of the S_0 and A_0 mode packets computed from the theoretical group velocity curves (see Fig. 7) over a distance of 40 mm and for a frequency-thickness product of $1.0 \text{ mm} \cdot \text{MHz}$ (where the plate's thickness is 3.0 mm and the excitation frequency is 0.333 MHz) are approximately 8 and 13 μs , respectively. Because the top and bottom horizontal stiffeners and bulkhead boundaries are in close proximity, reflections are present in the measured response arriving as early as 12 to 18 μs after the direct waves for Sensors 3 and 4. To attempt to discern the direct S_0 and A_0 wave modes and reflections for frequency-thickness products less than 1.8, a tuning approach is taken, which is discussed next.

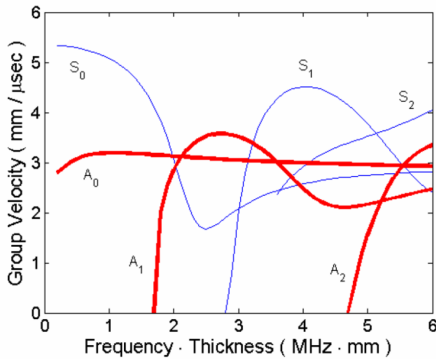


Figure 7: Theoretical group velocity curves for a 3mm thick al. plate

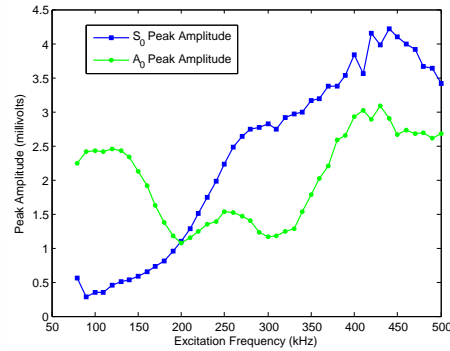


Figure 8: Measured absolute peak amplitude of the S_0 and A_0 modes as a function of frequency for a 3mm thick al. plate

By selecting the excitation frequency for a fixed transducer diameter (6.35 mm), the S_0 and A_0 modes can effectively be tuned, meaning that the modes with a relatively higher amplitude can be selected [Giurgiutiu (2005)]. Figure 8 shows the measured absolute peak amplitude of the S_0 and A_0 modes as a function of frequency from an experiment conducted by Underwood [Underwood (2008)]. By using two PZT

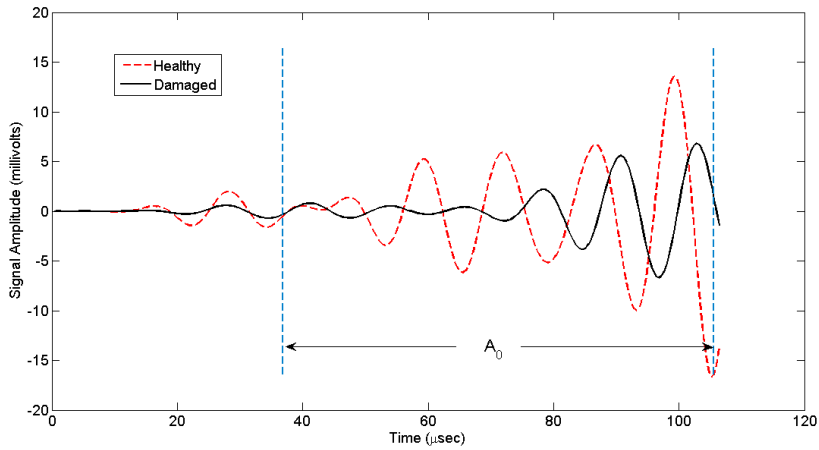
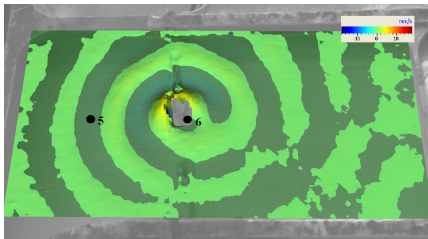
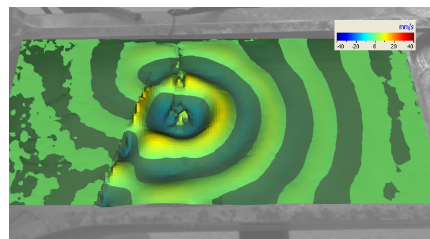


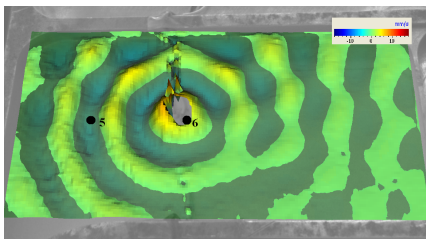
Figure 9: Measured response at Sensor 5 from a 80 kHz excitation signal from Sensor 6 for both a healthy and damaged structure



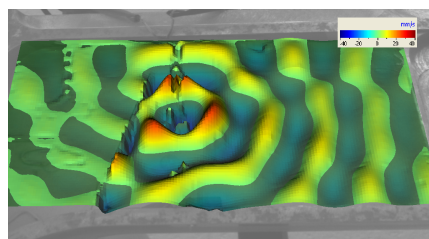
(a) Healthy - 46 μ s



(b) Damaged - 46 μ s



(c) Healthy - 70 μ s



(d) Damaged - 70 μ s

Figure 10: Out-of-plane velocity for a 80 kHz excitation

sensors 287 mm apart in the center of a 24 in x 48 in x 1/8 in thick aluminum test plate and knowing the arrival times of the direct S_0 waveform, the direct A_0 waveform, and the first reflections of each waveform, Underwood measured the peak amplitudes of each waveform without interference between modes. From

Fig. 8, an excitation frequency of 80 kHz was selected because the A_0 mode is dominant and 250 kHz was selected because the S_0 mode is larger in magnitude than the A_0 mode and is within the frequency range that the laser vibrometer could accurately measure.

Figure 9 shows the response signals collected at Sensor 5 from a 80 kHz excitation signal applied at Sensor 6 for both the healthy and damaged structures. The theoretical time of arrival window for the A_0 packet is shown as vertical dashed lines. Figures 10(a) through 10(d) show laser vibrometry scan data of both the healthy and damaged test articles at 46 and 70 μs being excited by a 80 kHz signal which excites primarily the A_0 mode. Sensors 5 and 6 are drawn in their approximate locations as black dots and labeled in Figs. 10(a) and 10(c). The primary difference between the healthy and damaged scan data at 46 μs , as shown in Figs. 10(a) and 10(b), is that the Lamb waves must first reflect off the upper horizontal stiffener in order to reach Sensor 5. These reflected waves can also be seen in Figure 9; however, the reflected waves have a longer time delay and significantly lower amplitude when compared to signals collected from the healthy or undamaged structure. One can also see in Fig. 10(b) that waves reflect off the simulated crack resulting in interference patterns that are apparent in Fig. 10(d). Figure 10(c) shows the healthy response at 70 μs where one can see that the waves reflecting from the upper and lower horizontal stiffeners create interference patterns which can make signal interpretation difficult.

Figure 11 shows the response signals collected at Sensor 5 from a 250 kHz excitation signal applied at Sensor 6 for both the healthy and damaged structures. The theoretical time of arrival window for the S_0 packet is also shown as vertical dashed lines. Figures 12(a) through 12(d) show laser vibrometry scan data of both the healthy and damaged test articles at 25 and 47 μs being excited by a 250 kHz signal which excites primarily the S_0 mode. Sensors 5 and 6 are drawn in their approximate locations as black dots and labeled in Figs. 12(a) and 12(c). Like the signal differences seen previously in the 80 kHz data, the differences between the signals collected from the healthy and damaged structures are clearly visible at 25 μs , as shown in Figs. 12(a) and 12(b). Primarily, the waves must reflect off the upper horizontal stiffener in order to reach Sensor 5. The reflected waves that propagate around the damage, as can be seen in Fig. 11, are similar to the direct waves but occur approximately 30 μs after the direct waves and have significantly less amplitude. One can also see in Fig. 12(b) waves reflecting off the simulated crack and combining with other waves to create interference patterns which are apparent in Fig. 12(d). In the healthy and damaged responses, as shown in Figs. 12(c) and 12(d), one can see that the reflected waves from the upper and lower horizontal stiffeners also create interference patterns. These interference patterns can

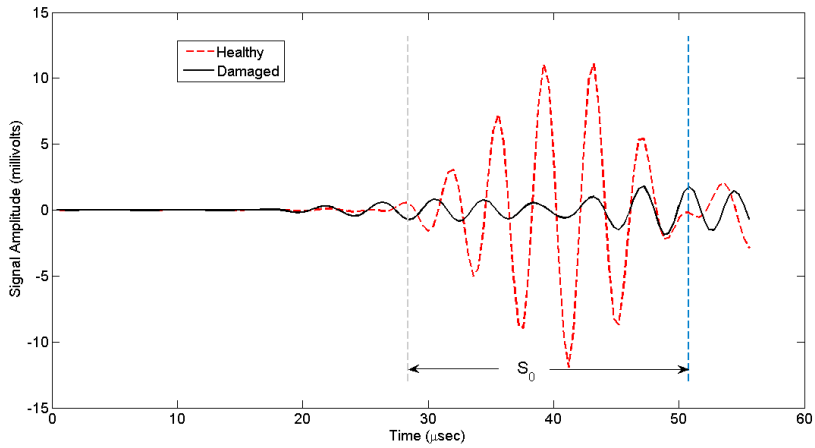


Figure 11: Measured response at Sensor 5 from a 250 kHz excitation signal from Sensor 6 for both a healthy and damaged structure

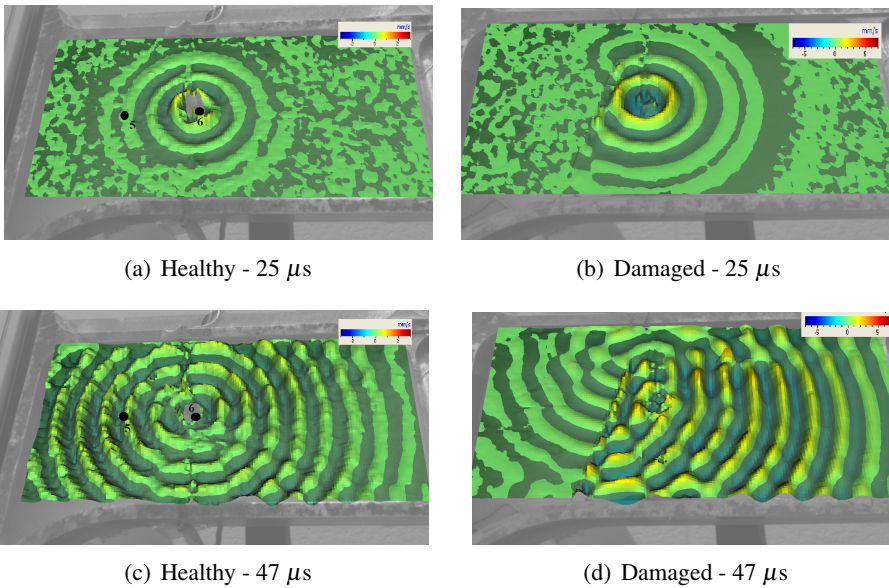


Figure 12: Out-of-plane velocity for a 250 kHz excitation

make signal interpretation difficult which provides further justification for using a windowing approach to exclude reflections. Overall, the laser scan data for both excitation frequencies clearly show how a simulated crack reflects Lamb waves and how Lamb waves reflect off the upper horizontal stiffener around the damage.

Figure 9 shows a decrease in amplitude in the A_0 mode as the simulated damage (EDM cuts) progresses up through the vertical stiffener between Sensors 5 and 6. Similarly, there is a noticeable decrease in amplitude in the S_0 mode shown in Fig. 11. Similar results are seen, but not shown here, when evaluating the responses measured at Sensors 2 and 4 when exciting the structure from Sensors 1 and 3, respectively. Therefore, crack length can be roughly estimated by comparing decreases in peak amplitude from the signals collected from the piezoelectric sensors at either 80 or 250 kHz. An alternative approach to evaluating signals at one excitation frequency is to evaluate responses over a much wider range of frequencies which is discussed next.

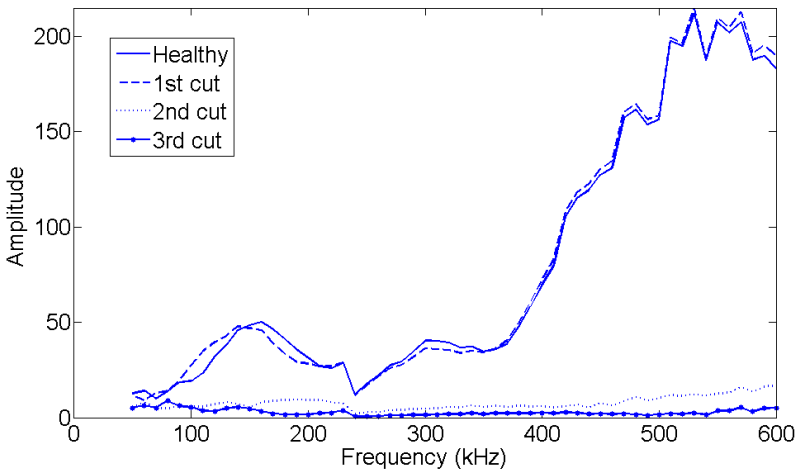


Figure 13: Amplitude versus excitation frequency for pitch-catch approach between Sensors 3 and 4 for healthy and damaged structure

Damage is detectable over a wide range of frequencies. The approach taken here is to use the previously discussed shortened theoretical arrival windows and select the appropriate window based on which mode is expected to dominate the response. Figures 13 and 14 compare the difference of the square root of the sum of the squares between healthy and damaged responses which is written as

$$Amplitude_i = \sqrt{\sum_{j=1}^m [healthy_{i,j} - measured_{i,j}]^2}. \quad (1)$$

The variables $healthy_{i,j}$ and $measured_{i,j}$ are the measured signals as shown in Figs. 9 and 11, m is the number of responses recorded in either the A_0 or S_0 response

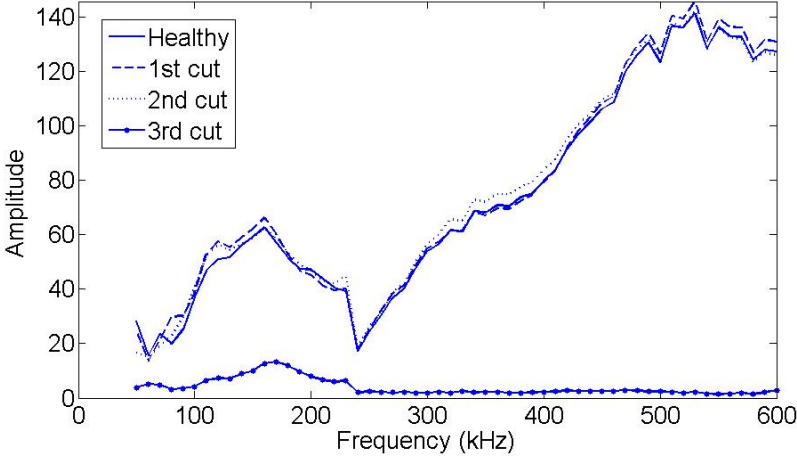


Figure 14: Amplitude versus excitation frequency for pitch-catch approach between Sensors 5 and 6 for healthy and damaged structure

window, $Amplitude_i$ values are shown in Figs. 13 and 14, and i is the frequency at which the amplitude is computed. The A_0 response window, as shown in Fig. 9, is used for excitation frequencies below 230 kHz, and the S_0 window, as shown in Fig. 11, is used for excitation frequencies 230 kHz and above. In Figs. 13 and 14, the jumps in amplitude at 230 kHz indicate where the evaluation windows change from the A_0 to the S_0 mode. A similar plot, not shown here, for Sensors 1 and 2 also shows that damage can easily be detected and a rough estimate of the simulated crack length can be made as the cut passes between the piezoelectric sensor pairs.

Using the mean square error as a damage index Q , where Q is defined as

$$Q = \frac{\sum_{i=1}^n \left[\frac{(healthy_i - measured_i)}{healthy_i} \right]^2}{n} \quad (2)$$

and n is the number of excitation frequencies, the values of Q in Table 1 show that the existence of damage can be quantified in a single value for each sensor pair. The frequency range for the damage index was further reduced to only use the S_0 response window, frequencies between 230 and 600 kHz, because the difference between damaged and healthy states is more distinct. Table 1 also shows that damage progress can be estimated by increases in the damage index from a value near zero, indicating there is little to no difference between the measured response and healthy response, to a value near one, indicating significant differences between the

Table 1: Values of the damage index Q for piezoelectric sensor pairs

Piezoelectric Sensor Pairs	EDM Cut 1	EDM Cut 2	EDM Cut 3
1 → 2	0.73048	0.74566	0.74082
3 → 4	0.00201	0.80899	0.93678
5 → 6	0.00060	0.00234	0.93256

healthy and measured responses.

4.2 Conclusion

Detecting damage using Lamb waves in a structure with restricted geometry requires that the piezoelectric sensors be placed in fairly close proximity to each other when using a pitch-catch approach. This close proximity results in the S_0 and A_0 packets arriving within several microseconds of each other, so a tuning approach is employed where excitation frequencies are selected to excite predominantly one mode. Additionally, only the response inside a conservatively short-duration time of arrival window determined for the dominant mode's group velocity is analyzed to ensure reflected waves are not sampled. Detecting simulated damage using EDM cuts to represent the crack is feasible for specific excitation frequencies. However, damage can also be detected over a wide range of frequencies when evaluating the responses in the dominant mode's theoretical arrival window. Using the mean square error between healthy and damaged responses as a damage metric, a simulated crack is shown to be detectable and an estimation of the crack length can be roughly approximated. Laser vibrometry measurements can provide significant insight into waveform interaction with the structure and damage. This insight should ultimately lead to better SHM system designs.

Acknowledgement: The authors would like to acknowledge Mr. Mark Derriso and Mr. Todd Bussey from the Air Force Research Labs (AFRL) and Dr. Martin DeSimio and Dr. Steven Olson from the University of Dayton Research Institute (UDRI) for their suggestions, encouragement, and expert help throughout this experiment. We would also like to thank Mr. David Currie from Warner Robbins AFB for his support in acquiring test articles. Finally, we would like to thank Mr. Jay Anderson from the Air Force Institute of Technology (AFIT) for his assistance in test setup.

References

- Crider, J.** (2007): Damage detection using Lamb waves for structural health monitoring. Master's thesis, Air Force Institute of Technology, 2007.
- Gao, W.; Glorieuxa, C.; Thoena, J.** (2003): Laser ultrasonic study of Lamb waves: Determination of the thickness and velocities of a thin plate. *International Journal of Engineering Science*, vol. 41, pp. 219–228.
- Giurgiutiu, V.** (2005): Tuned Lamb wave excitation and detection with piezoelectric wafer active sensors for structural health monitoring. *Journal of Intelligent Material Systems and Structures*, vol. 16, pp. 291–305.
- Hutchins, D.; Lundgren, K.; Palmer, S.** (1989): A laser study of transient Lamb waves in thin materials. *Journal of the Acoustical Society of America*, vol. 85, pp. 1441–1448.
- Kessler, S.** (2002): *Piezoelectric-based in-situ damage detection of composite materials for structural health monitoring systems*. PhD thesis, Massachusetts Institute of Technology, 2002.
- Kessler, S.; Amaratunga, K.; Wardle, B.** (2005): An assessment of durability requirements for aircraft structural health monitoring sensors. In *Proceedings of the 5th International Workshop on Structural Health Monitoring*.
- Kessler, S.; Shim, D.** (2005): Validation of a Lamb wave-based structural health monitoring system for aircraft applications. In *Proceedings of the SPIE's 12th International Symposium on Smart Structures and Materials*.
- Leong, W.; Staszewski, W.; Lee, B.; Scarpa, F.** (2005): Structural health monitoring using scanning laser vibrometry: III. Lamb waves for fatigue crack detection. *Smart Materials and Structures*, vol. 14, pp. 1387–1395.
- Lu, Y.; Ye, L.; Su, Z.; Yang, C.** (2008): Quantitative assessment of through-thickness crack size based on Lamb wave scattering in aluminum plates. *NDTE International*, vol. 41, pp. 59–68.
- Mal, A.** (2004): Structural health monitoring. *Mechanics*, vol. 33, pp. 6–28.
- Mallet, L.; Lee, B.; Staszewski, W.; Scarpa, F.** (2004): Structural health monitoring using scanning laser vibrometry: II. Lamb waves for damage detection. *Smart Materials and Structures*, vol. 113, pp. 261–269.
- Park, G.; Farrar, C.; Rutherford, C.; Robertson, A.** (2006): Piezoelectric active sensor self-diagnostics using electrical admittance measurements. *ASME Journal of Vibrations and Acoustics*, vol. 128, pp. 469–476.

Staszewski, W.; Lee, B.; Mallet, L.; Scarpa, F. (2004): Structural health monitoring using scanning laser vibrometry: I. Lamb wave sensing. *Smart Materials and Structures*, vol. 13, pp. 251–260.

Swenson, E.; Crider, J. (2007): Damage detection using Lamb waves for structural health monitoring on an aircraft bulkhead. In *Proceedings of the 6th International Workshop on Structural Health Monitoring*. Stanford University, CA.

Underwood, R. (2008): Damage detection analysis using Lamb waves in restricted geometry for aerospace applications. Master's thesis, Air Force Institute of Technology, 2008.